Hua et al. Nanoscale Research Letters (2018) 13:99
https://doi.org/10.1186/s11671-018-2476-7

Nanoscale Research Letters

NANO EXPRESS Open Access

Facile synthesis of surface-functionalized magnetic nanocomposites for effectively selective adsorption of cationic dyes

Yani Hua[1,2*], Juan Xiao[3], Qinqin Zhang[4], Chang Cui[1,2] and Chuan Wang[5*]

Abstract

A new magnetic nano-adsorbent, polycatechol modified Fe_3O_4 magnetic nanoparticles (Fe_3O_4/PCC MNPs) were prepared by a facile chemical coprecipitation method using iron salts and catechol solution as precursors. Fe_3O_4/PCC MNPs owned negatively charged surface with oxygen-containing groups and showed a strong adsorption capacity and fast adsorption rates for the removal of cationic dyes in water. The adsorption capacity of methylene blue (MB), cationic turquoise blue GB (GB), malachite green (MG), crystal violet (CV) and cationic pink FG (FG) were 60.06 mg g^{-1}, 70.97 mg g^{-1}, 66.84 mg g^{-1}, 66.01 mg g^{-1} and 50.27 mg g^{-1}, respectively. The adsorption mechanism was proposed by the analyses of the adsorption isotherms and adsorption kinetics of cationic dyes on Fe_3O_4/PCC MNPs. Moreover, the cationic dyes adsorbed on the MNPs as a function of contact time, pH value, temperature, coexisting cationic ions and ion strength were also investigated. These results suggested that the Fe_3O_4/PCC MNPs is promising to be used as a magnetic adsorbent for selective adsorption of cationic dyes in wastewater treatment.

Keywords: Adsorption, Polycatechol, Fe_3O_4, Magnetic adsorbent, Selectivity

Background

Inorganic and organic wastes produced by human activities have resulted in high volumes of contaminated waters which threaten the health of human beings and other living organisms [1]. Water pollution is one of the most serious environmental problems nowadays, which hinders the development of human society [2, 3]. In particular, dye pollutants have attracted wide concerns from the public because of the high visibility and the toxic impact on biological organisms and the ecology [4]. Organic dyes have been extensively used in various branches such as textile, paper, printing, color photography, pharmaceutical industry, leather, cosmetics, plastic and other industries, which have been the major industrial wastewater sources [5]. The quantity of dye wastewater is extremely large, generally, the volume of discharged wastewater from each step of a textile operation is approximately at a high rate of between 40 L/kg and 65 L/kg of the product [6]. In addition, dyes are non-biodegradable substances that remain stable under different conditions due to their synthetic origin and complex aromatic structures [7]. Therefore, it is necessary to select an appropriate method to remove dyes from wastewater before discharging into the environment.

In recent years, a variety of techniques has been used to treat dye wastewater including photocatalytic degradation [8], coagulation [9], electrochemical processes [10], chemical oxidation [11], membrane filtration [12], biological treatment [13] and adsorption [14]. Among these dye wastewater treatment techniques, adsorption has been widely used due to their merits of simplicity, high efficiency and economy [15, 16]. Many adsorbents such as activated carbon, kaolin, montmorillonite clay, waste red mud, fullers earth and fired clay have been reported to decolorize wastewater [17, 18]. Especially, magnetic nanoparticles (MNPs) have attracted considerable attention as adsorbent materials for organic dyes and heavy metals, due to their unique magnetic properties, low cost, biocompatible, easily synthesized, readily recycle, particularly economic and environmental friendly [19]. Several methods have been developed to synthesize magnetic Fe_3O_4 nanoparticles, including i)

* Correspondence: 707837380@qq.com; cuichang@cigit.ac.cn
[1]Key Laboratory of Reservoir Aquatic Environment, Chongqing Institute of Green and Intelligent Technology, Chinese Academy of Sciences, Fangzheng Avenue, number 266, Beibei District, Chongqing 400714, China
[5]School of Environmental Science and Engineering, Guangzhou University, Guangzhou 510006, China
Full list of author information is available at the end of the article

coprecipitation of ferrous and ferric aqueous solution in the presence of a base [20]; ii) thermal decomposition of an iron complex [21]; iii) sonochemical approach [22].

Because of their high surface energies and intrinsic magnetic interactions, easy aggregation of Fe_3O_4 MNPs would reduce their surface/volume ratio and dispersion stability in aqueous solution [23]. The stabilizers such as surfactants, supporters, oxides or polymeric compounds have been used to modify Fe_3O_4 MNPs to increase their stability and improve their dispersity. Zhang et al. synthesized magnetic Fe_3O_4/C core shell nanoparticles and used as absorbents performing good adsorption capacity for dye removal [24]. Wang et al. prepared Fe_3O_4 nanoparticles with cetyltrimethylammonium bromide (CTAB) assistant for adsorption removal of congo red (CR) and methylene blue (MB) [25]. Furthermore, the adsorption capacity of bare Fe_3O_4 MNPs is not strong enough.

In order to improve the adsorption property, surface functionalization of Fe_3O_4 MNPs has been studied. Zhang et al. modified Fe_3O_4 MNPs with 3-glycidoxypropyltrimethoxysilane (GPTMS) and glycine (Gly), the magnetic nanocomposites could excellently remove both anionic and cationic dyes in severe environment (highly acidic or strong alkaline) [26]. Moreover, selective adsorption can be greatly improved for the enrichment of pollutants due to introduction of large numbers of active sites. Pourjavadi et al. reported a new functionalized magnetic nanocomposite of poly(methylacrylate) for the efficient removal of anionic dyes from aqueous media [27]. Polycatechol, resulting from the polymerization of catechol catalyzed by Fe(III) [28–30], has been exploited in surface modifications as adhesives and coatings over a wide range of both organic and inorganic materials due to their unique thermal, structural properties, and the ability to form stable complexes with metal oxides [31, 32]. It means that Fe_3O_4 MNPs modified with polycatechol will greatly increase the adsorption ability of Fe_3O_4 MNPs. However, there is no report about polycatechol modified Fe_3O_4 MNPs as an absorbent for dye removal by far.

In this work, polycatechol modified Fe_3O_4 MNPs (Fe_3O_4/PCC MNPs) were prepared by a facile coprecipitation method and used as adsorbents for dye removal. The absorbent was characterized using magnetic hysteresis loops, thermogravimetric analysis and zeta potential analysis technique. Five kinds of cationic dyes, including methylene blue (MB), cationic turquoise blue GB (GB), malachite green (MG), crystal violet (CV) and cationic pink FG (FG), were chosen as the model compounds to expose the adsorption behavior of Fe_3O_4/PCC MNPs. The adsorption kinetics, isotherm analyses and the effect of different experimental conditions on the removal of cationic dyes were also investigated.

Methods

Materials

Ferric chloride ($FeCl_3{\cdot}6H_2O$), ferrous sulfate ($FeSO_4{\cdot}7H_2O$), ammonium hydroxide ($NH_3{\cdot}H_2O$, 25%), MB, GB, MG, CV, FG, Orange II, Fuchsin, methyl orange (MO) and catechol were obtained from Chuandong Chemical Inc., Chengdu, Sichuan, China. All chemicals were analytical grade and used without further purification and all solutions and suspensions were prepared with deionized water. The structures of five cationic dyes, including MB, GB, MG, CV and FG, were shown in Fig. 1.

Preparation and characterization of Fe_3O_4/PCC MNPs

Fe_3O_4/PCC MNPs were prepared by a facile chemical coprecipitation method using iron salts and catechol as precursors [23]. The whole synthesis process was performed at ambient atmosphere. In brief, $FeCl_3{\cdot}6H_2O$ (10 mmol) and $FeSO_4{\cdot}7H_2O$ (5 mmol) were dissolved into 75 mL deionized water, then mixed with 75 mL of catechol (20 mM) sufficiently. When catechol was mixed with iron solution (pH 2.87), the polymerization of catechol catalyzed by Fe^{3+} happened, forming polycatechol, which was black coarse precipitates [30]. Simultaneously, Fe^{3+} ions were chemically adsorbed on polycatechol through complexation and served as nucleation precursors. The mixture was standing for 30 min and then was added into 100 mL of ammonium hydroxide (3.3 M) rapidly, aging for 120 min under vigorous stirring. The magnetic nanoparticles in situ grew to form aggregations on the surface of polycatechol chains. Couples of Fe_3O_4/PCC chains combined with each other tightly to form Fe_3O_4/PCC MNPs. The whole synthesis processes were performed at ambient atmosphere, without any protective atmosphere. The black magnetic nanoparticles were separated by an external magnet and washed with deionized water until neutral pH and dried in a vacuum oven at 50 °C for 24 h. Fe_3O_4 MNPs were synthesized with the same procedures as mentioned above without adding catechol. All the products were stored in a desiccator under ambient temperature for further experiments.

Magnetic properties were measured at room temperature on a magnetic property measurement system (MPMS XL-7, Quantum Design, America). Thermogravimetric analysis (TGA) was carried out for powder samples using a TGA/DSC 1 thermogravimetric analyzer (TGA) (Mettler-Toledo, Switzerland) under N_2 environment at a heating rate of 5 °C min^{-1}. The zeta potentials of catalyst suspensions at different pH were determined by a Malvern 3000 Zetasizer.

Batch adsorption experiments

Sorption isotherm experiments were carried out by shaking 25 mg Fe_3O_4/PCC MNPs in 25 mL solution with varied adsorbates, with initial adsorbate concentration varying

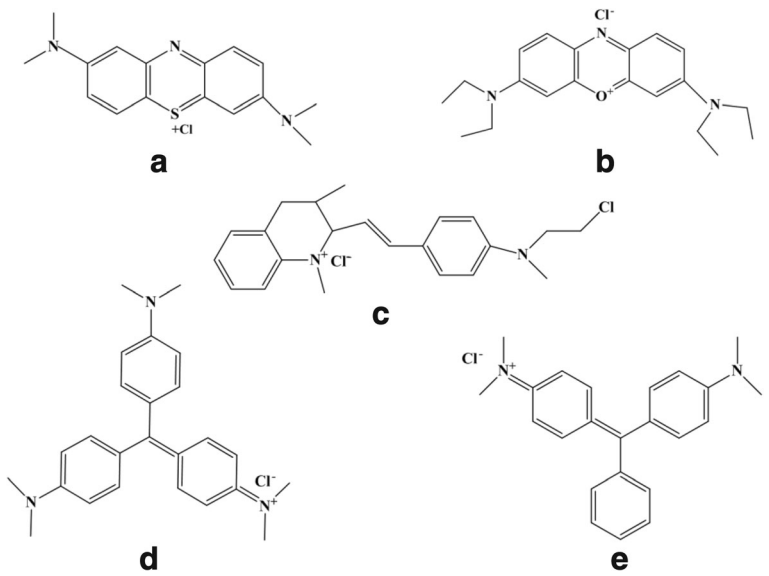

Fig. 1 Molecular structures of (**a**) MB (**b**) GB (**c**) MG (**d**) CV (**e**) FG. As shown as Fig. 1, the structure of five kinds of cationic dyes are described

from 0.02 mM to 0.4 mM. The mixture was continuously shaken on a shaker at 180 rpm under controlled temperature of 30 °C until reaching equilibrium. The solution pH was adjusted by using 1.0 M H_2SO_4 or 1.0 M NaOH solutions. After adsorption, the adsorbent was separated from the solution under magnetism, and then the supernatant liquid was measured at the maximum absorbance of each dye by a UV-vis spectrophotometer.

Furthermore, the adsorption kinetics of the processes were studied. 100 mg Fe_3O_4/PCC MNPs were suspended into 100 mL 0.1 mM solutions of adsorbates, and then shaken at 180 rpm under pH 6.0 and 30 °C. At different time intervals, 0.5 mL of suspension sample was withdrawn and immediately separated by an external magnetism and the supernatant liquid was collected for analysis.

The influences of pH value and temperature on adsorption of cationic dyes were also studied. The typical batch adsorption experiment was carried out as follows: 50.0 mg of Fe_3O_4/PCC MNPs was dispersed in 50.0 mL of cationic dyes solution and then was shaken on a shaker with a speed of 180 rpm.

All the adsorption experiments were carried out in duplicate. The adsorption capacity of each dye in the adsorption system, q_e, was calculated according to Eq. (1):

$$q_e = (C_i - C_e)\, V/M_s \quad (1)$$

Where q_e (mg g^{-1}) is the adsorption capacity, C_e (mM) is the equilibrium concentration in the aqueous phase, Ci (mM) is the initial aqueous phase concentration, V (L) is the volume of solution and M_s (g) is the mass of solid adsorbent.

Results and discussion

Characterization of Fe_3O_4/PCC MNPs

Figure 2a shows the magnetic hysteresis loops determined at room temperature for Fe_3O_4 and Fe_3O_4/PCC MNPs. The saturation magnetization values of Fe_3O_4/PCC MNPs were 53.5 emu g^{-1}, higher than that of Fe_3O_4 (49.6 emu g^{-1}), suggesting that they could be easily separated by an external magnetic field [33]. The particle size, spin canting phenomenon, size effect, and others, are related to the saturation magnetization of the ferrite nanoparticles [34]. The modification of polycatechol makes the Fe_3O_4/PCC MNPs much higher in crystallization, and smaller in particle size than Fe_3O_4 MNPs, which could be result in the higher saturation magnetization of Fe_3O_4/PCC MNPs than Fe_3O_4 MNPs. Furthermore, higher saturation magnetization of the prepared Fe_3O_4/PCC MNPs could also be attributed to the surface effect, sometimes called the "dead surface". The dead surface is associated with disorder of surface spin [35].

The thermal behaviors of Fe_3O_4 and Fe_3O_4/PCC MNPs were further investigated by thermogravimetric analysis (TGA) (Fig. 2b). For the TGA curve of Fe_3O_4 MNPs, the weight loss (6.5%) below 150 °C was due to the loss of physically adsorbed water. For the curve of Fe_3O_4/PCC MNPs, the weight loss (5.2%) below 150 °C was due to the loss of physically adsorbed water, the weight loss (9.4%) from 150 °C to 400 °C was ascribed to the loss of oxygen-containing functional groups, the weight loss (6.8%) from 400 °C to 800 °C was mainly attributed to the burning of carbon, and a slight weight gain (2.3%) over 800 °C was due to the oxidization of Fe_3O_4 to γ-Fe_2O_3 [36]. The Fe_3O_4/PCC MNPs exhibited a lower thermal stability

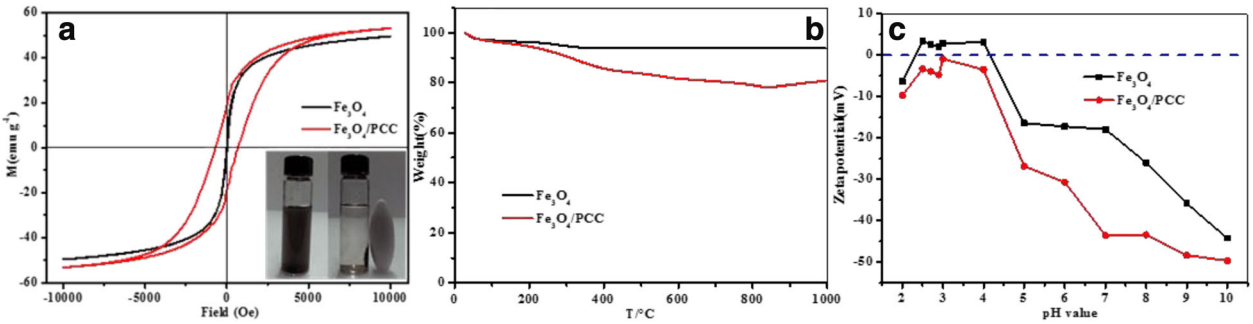

Fig. 2 **a** Magnetization behavior of Fe_3O_4 MNPs and Fe_3O_4/PCC MNPs at room temperature. **b** Thermogravimetry (TGA) curves of Fe_3O_4 MNPs and Fe_3O_4/PCC MNPs. **c** zeta potentials of Fe_3O_4/PCC magnetic nanoparticles. In Fig. 2, the blank lines represent the nature of Fe_3O_4 MNPs, and the red lines are on behalf of the property of Fe_3O_4/PCC MNPs

rather than Fe_3O_4, due to the modification of polycatechol [37].

Figure 2c shows the zeta potentials of the Fe_3O_4 and Fe_3O_4/PCC suspensions at various pH values. As shown in Fig. 2c, the isoelectric point of Fe_3O_4 was 4.2, while the surface of Fe_3O_4/PCC MNPs possessed negative charges in the pH range of 3.0–10.0, which could be due to the electronegativity of phenolic hydroxyl group in polycatechol. Moreover, the surface charge density of Fe_3O_4/PCC MNPs increased as the pH increased from 3.0 to 10.0. The negative charges of Fe_3O_4/PCC MNPs also prevented nanoparticles from agglomeration.

Selective adsorption of Fe_3O_4/PCC MNPs

The adsorption properties of the Fe_3O_4/PCC MNPs towards cationic dyes, anionic dyes and phenol from aqueous solution were investigated in detail. Figure 3 shows the removal efficiencies of MB as a kind of cationic dye, MO as a kind of anionic dye and phenol adsorbed onto Fe_3O_4/PCC MNPs. It was observed that the removal efficiency of MB was 75.7%. However, the removal efficiencies of MO was 10.9% only, and the removal efficiency of phenol was 1.5% only. The results indicated that the Fe_3O_4/PCC MNPs selectively adsorbed cationic dye, due to the electrostatic interaction (Fig. 2c).

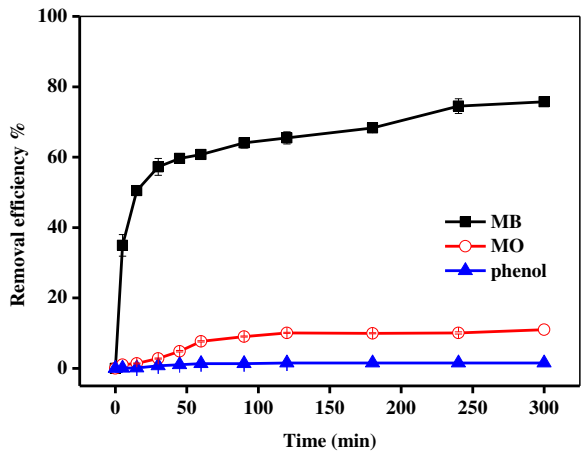

Fig. 3 The removal efficiency of MB, MO and phone adsorbed by Fe_3O_4/PCC MNPs. As shown as Fig. 3, the blank line represent the removal efficiency of MB, the red line reperesent the removal of MO, and the blue line represent the removal of phonel

Adsorption kinetics of cationic dyes

Adsorption kinetics of five cationic dyes on Fe_3O_4/PCC MNPs were studied using two kinetic models, namely the pseudo-first-order model and the pseudo-second-order model (Fig. 3). In the pseudo-first-order kinetic model, the rate constant of dyes adsorption is expressed as [38]:

$$Ln(q_e - q_t) = \ln(q_e) - k_1 t \quad (2)$$

where q_e and q_t are the amounts of dyes adsorbed (mg g^{-1}) at equilibrium and at any instant of time t (min), respectively, and k_1 is the rate constant of pseudo-first-order adsorption (min^{-1}).

The pseudo-second-order kinetic model is described by the formula [39]:

$$t/q_t = 1/k_{ad}\, q_e^{\,2} + 1/q_e \quad (3)$$

Where q_e and q_t are, respectively, the amount of dyes adsorbed at the equilibrium and time t (mg g^{-1}); and k_{ad} is the pseudo-second-order rate constant for the adsorption process (mg g^{-1} min^{-1}). The parameter values for each model were calculated from the linear least square method and the correlation coefficients were presented in Table 1. The results showed that all the adsorption kinetics of these five cationic dyes on Fe_3O_4/PCC MNPs could be well described by pseudo-second-order kinetics model with high correlation coefficient ($R^2 > 0.997$) and the rate constants (k_{ad}) were calculated to 0.043, 0.047,

Table 1 Kinetics parameters for the adsorption of cationic dyes on Fe_3O_4/PCC MNPs

Cationic dyes	pseudo-first-order kinetics			pseudo-second-order kinetics		
	q_e	k	R^2	q_e	k	R^2
MB	11.83	0.0048	0.859	23.12	0.043	0.999
GB	20.17	0.0024	0.798	21.26	0.047	0.997
MG	12.28	0.0041	0.868	19.61	0.051	0.998
CV	7.71	0.0038	0.682	17.57	0.057	0.999
FG	17.92	0.0030	0.873	19.38	0.052	0.998

0.051, 0.057, 0.052 g mg^{-1} mL^{-1}, corresponding to MB, GB, MG, CV and FG, respectively (Fig. 4 and Table 1). Moreover, the adsorption capacity of MB on Fe_3O_4/PCC MNPs was significantly improved, comparing to that of Fe_3O_4 MNPs (Additional file 1: Figure S1). The main reason was the electrostatic attractions between the positive charge of cationic dyes and the negative charge of Fe_3O_4/PCC MNPs.

Adsorption isotherms of different cationic dyes

The adsorption isotherm played a significant role in evaluating the adsorption properties of Fe_3O_4/PCC MNPs [40]. To depict the adsorption process thoroughly, two well-known isotherm equations, Langmuir and Freundlich equations (Eqs. (4) and (5)), were applied [41].

Langmuir equation:

$$C_e/q_e = C_e/q_m + 1/K_L\, q_m \tag{4}$$

where q_e (mg g^{-1}) is the equilibrium adsorption capacity of dye on the adsorbent; C_e (mg L^{-1}) is the equilibrium dye concentration in solution; q_m (mg g^{-1}), the maximum capacity of the adsorbent; and K_L (L mg^{-1}), the Langmuir constant.

Freundlich equation:

$$q_e = K_F\, C_e^{1/n} \tag{5}$$

Where q_e and C_e are defined to be the same as above; K_F (L mg^{-1}) is the Freundlich constant; and n is the heterogeneity factor.

Figure 5 shows the adsorption isotherms of cationic dyes on Fe_3O_4/PCC MNPs. The results indicated that the adsorption of the five cationic dyes all fitted better with Langmuir equation than with Freundlich equation according to the correlation coefficients. The maximum adsorption capacities (q_m) for these dyes were worked out by the Langmuir equation which were listed in Table 2. The q_m for cationic dyes: MB, GB, MG, CV and FG were 60.06, 70.97, 66.84, 66.01 and 50.27 mg g^{-1}, respectively. The fitted Langmuir model assumed that the single pollutant bonded to a single site on the adsorbent and that all surface sites on the adsorbents had the same affinity for pollutant and no interactions between pollutant [42].

Effect of temperature on cationic dyes adsorption

The effect of temperature on the adsorption of cationic dyes was shown in Fig. 6. As can be seen, the removal efficiency of MB increased with rising temperature (30–45 °C), and it reached up to 84% at 45 °C, which suggested that the adsorption of MB on Fe_3O_4/PCC was an endothermic process. While the removal efficiency of GB and CV decreased with rising temperature, suggesting an exothermic reaction for the adsorption of GB and CV, which indicated the sorption processes were mainly physical adsorption. Furthermore, the reaction temperature had little effect on the adsorption of WG and FG. The effect of reaction temperature on the adsorption of five cationic dyes was different, mainly because of the different structure of dyes and the hole of the MNPs. When the holes of the MNPs are too small to be get into, the adsorbate molecules have to go over the high barrier to get into

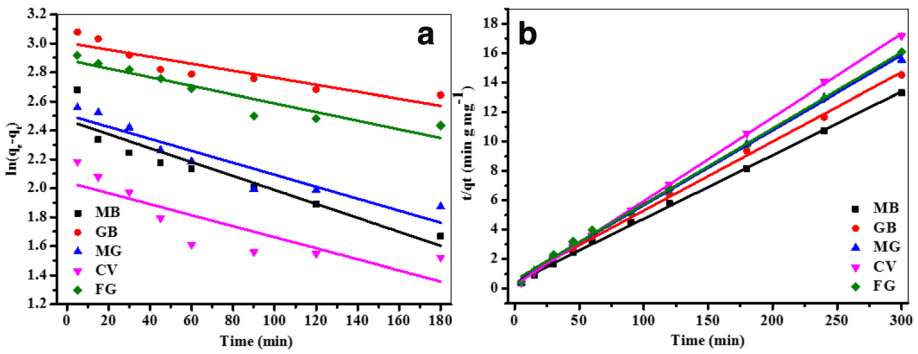

Fig. 4 Adsorption of cationic dyes on Fe_3O_4/PCC MNPs (**a**) pseudo-second-order kinetics (**b**) pseudo-first-order kinetics. As shown as Fig. 4, the blank line represent the adsorption of MB, the red line reperesent the adsorption of GB, the blue line represent the adsorption of MG, the magenta represent of CV adsorption, and the olive is on behalf of the adsorption of FG

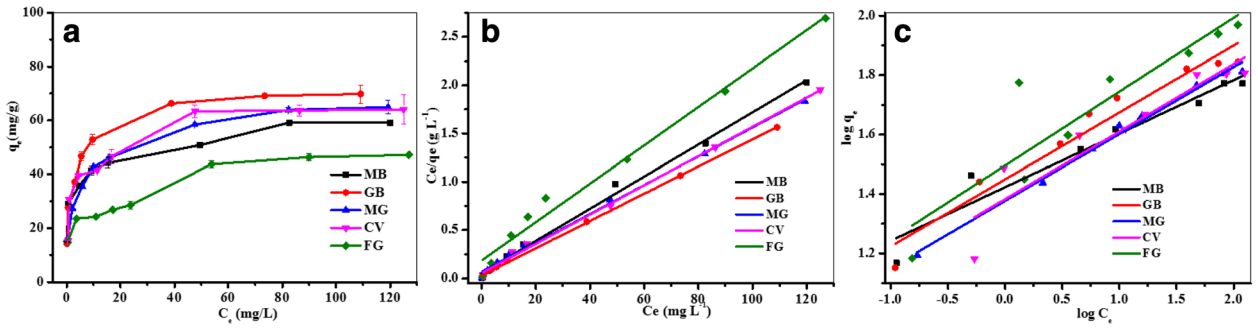

Fig. 5 **a** Isotherms of cationic dyes adsorption on Fe_3O_4/PCC MNPs (**b**) Langmuir and (**c**) Freundlich adsorption isotherm models for organic dyes by Fe_3O_4/PCC MNPs. As shown as Fig. 5, the blank line represent the adsorption of MB, the red line reperesent the adsorption of GB, the blue line represent the adsorption of MG, the magenta line represent of CV adsorption, and the olive line is on behalf of the adsorption of FG

the hole. Since the holes are small and the diffusion is blocked, the adsorption process is more unstable, resulting in higher energy and the process is endothermic. Otherwise the process is exothermic.

Effect of pH on cationic dyes adsorption

The pH of the aqueous solution was an important factor that affects the dye-adsorption process, because it influenced the surface charge of an adsorbent and the ionization behavior of both the adsorbent and dye [43]. The effect of pH on the removal of cationic dyes was studied at a dye concentration of 0.1 mM at 30 °C and at pH values from 3.0 to 9.0. As shown in Fig. 7, the removal efficiency of cationic dyes increased with increasing pH value. Because the Fe_3O_4/PCC MNPs possessed negative charge, and their surface charge density increased with higher pH (Fig. 2c), cationic dyes were adsorbed on Fe_3O_4/PCC MNPs through the electrostatic attractions between the positive charge of cationic dyes molecules and the negative charge of Fe_3O_4/PCC MNPs. As the pH increases, the electrostatic attraction between the negatively charged surface of the Fe_3O_4/PCC composite and cationic dyes molecule increased, resulting in the increase in the adsorption capacity of cationic dyes. Therefore, the elevated pH helped the removal of cationic dyes by Fe_3O_4/PCC MNPs.

Table 2 Parameters of adsorption isotherm models parameters for the adsorption of dyes on Fe_3O_4/PCC MNPs

Cationic dyes	Langmuir model			Freundlich model		
	q_e	b	R^2	q_e	n	R^2
MB	60.06	0.31	0.995	26.48	5.54	0.928
GB	70.97	0.47	0.999	28.12	4.43	0.943
MG	66.84	0.22	0.997	23.81	4.44	0.990
CV	66.01	0.28	0.997	24.14	4.39	0.852
FG	50.27	0.34	0.983	31.33	4.02	0.796

Effect of coexisting cations on MB adsorption

Dye effluents always contained a large variety of coexisting ions, which might affect the dye adsorption process [4]. In this study, three commonly coexisting salts, NaCl, $MgSO_4$ and $FeCl_3$ were selected to study the effect of coexisting

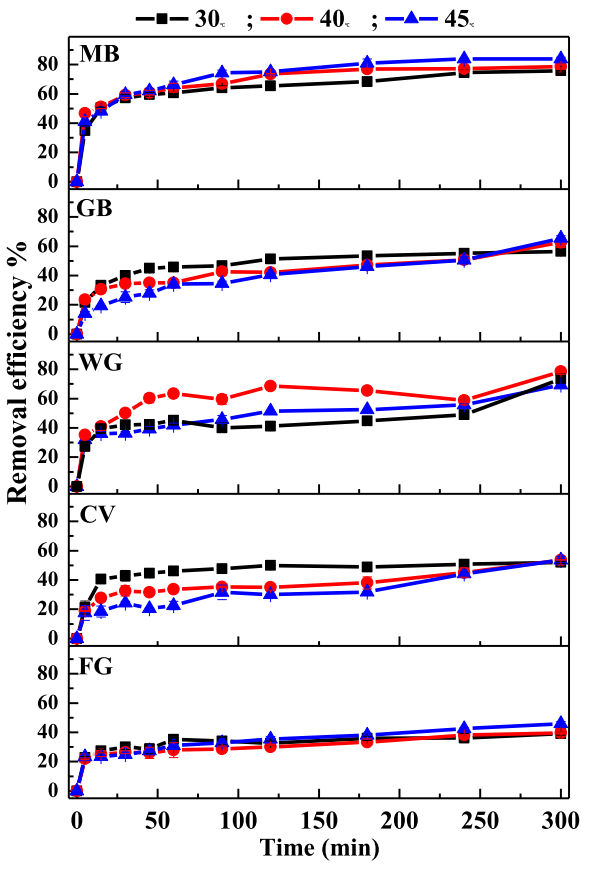

Fig. 6 Effect of temperature on the adsorption of cationic dyes on Fe_3O_4/PCC MNPs. As shown as Fig. 6, the blank line represent that the temperature is 30 °C, the red line reperesent that the temperature is 40 °C, and the blue line represent the temperature is 45 °C

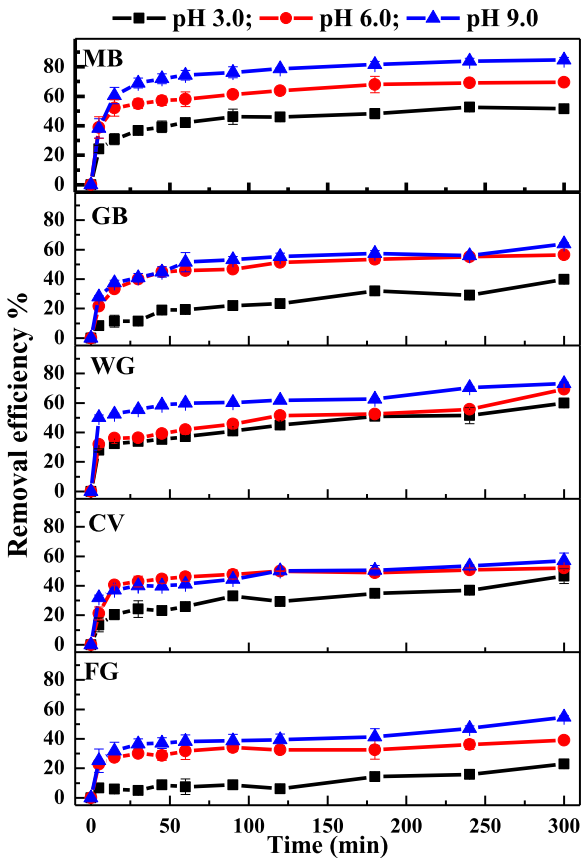

Fig. 7 Effect of initial pH on the removal of cationic dyes on Fe_3O_4/PCC MNPs the temperature is 30 °C. As shown as Fig. 7, the blank line represent that the solution pH is 3.0, the red line reperesent that the solution pH is 6.0, and the blue line represent that the solution pH is 9.0

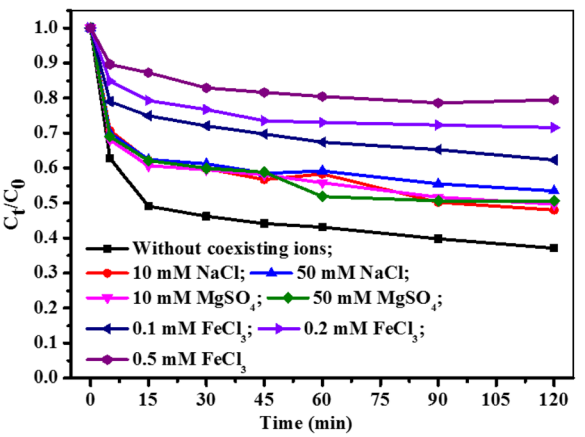

Fig. 8 Effect of coexisting cations and ionic strength on the adsorption of MB on Fe_3O_4/PCC MNPs. As shown as Fig. 8, the blank line represent the adsorption of MB without any coexisting ions, the red line reperesent the effect on MB adsorption with 10 mM NaCl, the blue line reperesent the effect on MB adsorption with 50 mM NaCl, the magenta line reperesent the effect on MB adsorption with 10 mM $MgSO_4$, the olive line reperesent the effect on MB adsorption with 50 mM $MgSO_4$, the navy line reperesent the effect on MB adsorption with 0.1 mM $FeCl_3$, the violet line reperesent the effect on MB adsorption with 0.2 mM $FeCl_3$, the purple line reperesent the effect on MB adsorption with 0.1 mM $FeCl_3$

cations and their ionic strength on MB adsorption onto Fe_3O_4/PCC MNPs with the results presented in Fig. 8. As can be seen, Na^+, Mg^{2+} and Fe^{3+} all suppressed MB adsorption due to the competition adsorption between cations and MB on the adsorptive sites of Fe_3O_4/PCC MNPs. Moreover, the removal efficiency of MB decreased from 63% to 20% with Fe^{3+} concentration increasing from 0.1 mM to 0.5 mM. Such competitive adsorption was widely reported in the literature [44]. The results further confirmed the electrostatic adsorption of MB on Fe_3O_4/PCC MNPs.

Recycle of the adsorbent

After adsorption, Fe_3O_4/PCC MNPs could be regenerated with ethanol desorption at pH 4.0 for 12 h and washed with deionized water to neutral condition. The Fe_3O_4/PCC MNPs could be regenerated and reused for five times. Figure 9 shows the adsorption performance of the regenerated Fe_3O_4/PCC MNPs for cationic dyes. The removal efficiency of cationic dyes decreased gradually during the first adsorption-desorption cycle to the fifth cycle. At the sixth cycle, the removal efficiency of MB, GB, MG, CV and FG decreased dramatically to 27%, 23%, 37%, 43% and 39%, respectively. Notably, the presence of magnetic nanoparticles facilitated separation and recovery of the adsorbent. It indicates that the Fe_3O_4/PCC MNPs has a certain economic feasibility.

Conclusion

In conclusion, a new magnetic nano-adsorbent (Fe_3O_4/PCC MNPs) was successfully prepared with active adsorption

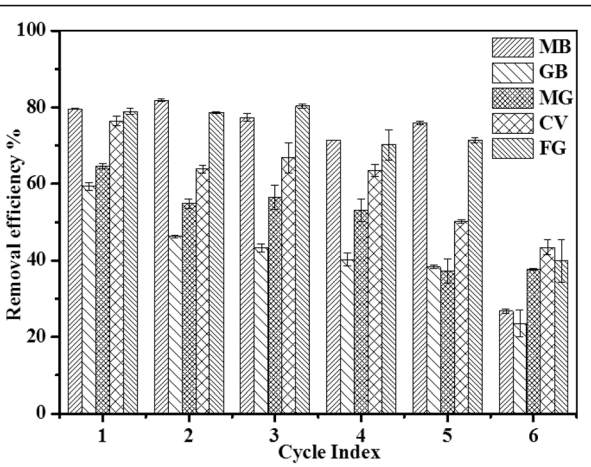

Fig. 9 The histogram of removal efficiency of cationic dyes by Fe_3O_4/PCC MNPs adsorption ([Fe_3O_4/PCC] = 1.0 g L^{-1}, $[dyes]_0$ = 0.1 mM, pH 6.0, t = 300 min)

sites for removing cationic dyes from aqueous solution. The introduction of polycatechol in the structure of Fe_3O_4/PCC MNPs performed amazing advantages, including preventing nanoparticles from agglomeration and improving adsorption behavior of the MNPs. The electrostatic interaction was found to be the main force of the adsorption behavior for the cationic dyes. The adsorption process was well-described by pseudo-second-order kinetics and Langmuir isotherm models, respectively. The results demonstrated that Fe_3O_4/PCC MNPs showed potential application for cationic dyes removal in industrial effluents.

Additional file

Additional file 1: Figure S1. Adsorption removal efficiency of MB on Fe3O4 and Fe3O4/PCC MNPs, inset is the adsorption capacity of MB ([Fe3O4/PCC] = 1.0 g L-1, [Fe3O4] = 1.0 g L-1, [MB] = 0.1 mM, pH = 6.0, T = 30 °C). (DOC 45 kb)

Abbreviations

CR: Congo red; CTAB: Cetyltrimethylammonium bromide; Fe_3O_4/PCC: Fe_3O_4/polycatechol; Gly: Glycine; GPTMS: 3-glycidoxypropyltrimethoxysilane; MB: Methylene blue; MNPs: Magnetic nanoparticles; PCC: Polycatechol; TGA: Thermogravimetric analysis

Acknowledgements

The authors include Chuan Wang thank Professor Liu for fruitful discussions.

Funding

Not applicable

Availability of data and materials

Not applicable

Authors' contributions

Juan Xiao participated in the materials preparation, data analysis and drafted the manuscript. Qinqin Zhang participated in the sample characterization. Chang Cui conceived and co-wrote the paper. Chuan Wang involved in the experimental design and revised the manuscript. All authors include Chuan Wang read and approved the final manuscript.

Competing interests

All the authors include Chuan Wang declare that they have no competing financial interests.

Publisher's Note

Author details

[1]Key Laboratory of Reservoir Aquatic Environment, Chongqing Institute of Green and Intelligent Technology, Chinese Academy of Sciences, Fangzheng Avenue, number 266, Beibei District, Chongqing 400714, China. [2]University of Chinese Academy of Sciences, Beijing 100049, China. [3]Guangdong Environmental Monitoring Center, Guangzhou 510308, China. [4]Yangtze Normal University, Chongqing 400714, China. [5]School of Environmental Science and Engineering, Guangzhou University, Guangzhou 510006, China.

Received: 16 October 2017 Accepted: 12 February 2018
Published online: 12 April 2018

References

1. Gupta VK, Suhas (2009) Application of low-cost adsorbents for dye removal - a review. J Environ Manag 90:2313–2342
2. Wu CH, Maurer C, Wang Y, Xue SZ, Davis DL (1999) Water pollution and human health in China. Environ Health Persp 107:251–256
3. Koshal RK (1976) Water-pollution and human health. Water Air Soil Poll 5:289–297
4. Konicki W, Sibera D, Mijowska E, Bielun ZL, Narkiewicz U (2013) Equilibrium and kinetic studies on acid dye acid red 88 adsorption by magnetic $ZnFe_2O_4$ spinel ferrite nanoparticles. J Colloid Interf Sci 398:152–160
5. Rahimi R, Kerdari H, Rabbani M, Shafiee M (2011) Synthesis, characterization and adsorbing properties of hollow Zn-Fe_2O_4 nanospheres on removal of Congo red from aqueous solution. Desalination 280:412–418
6. Vakili M, Rafatullah M, Salamatinia B, Abdullah AZ, Ibrahim MH, Tan KB, Gholami Z, Amouzgar P (2014) Application of chitosan and its derivatives as adsorbents for dye removal from water and wastewater: a review. Carbohyd Polym 113:115–130
7. Buthelezi SP, Olaniran AO, Pillay B (2012) Textile dye removal from wastewater effluents using bioflocculants produced by indigenous bacterial isolates. Molecules 17:14260–14274
8. Vaiano V, Iervolino G, Sannino D, Murcia JJ, Hidalgo MC, Ciambelli P, Navio JA (2016) Photocatalytic removal of patent blue V dye on au-TiO_2 and Pt-TiO_2 catalysts. Appl Catal B-Environ 188:134–146
9. Li H, Liu S, Zhao J, Feng N (2016) Removal of reactive dyes from wastewater assisted with kaolin clay by magnesium hydroxide coagulation process. Colloid Surf A Physicochem Eng Asp 494:222–227
10. Yahiaoui I, Benissad FA, Fourcade F, Amrane A (2016) Enhancement of the biodegradability of a mixture of dyes (methylene blue and basic yellow 28) using the electrochemical process on a glassy carbon electrode. Desalin Water Treat 57:12316–12323
11. Venkatesh S, Quaff AR, Pandey ND, Venkatesh K (2016) Decolorization and mineralization of CI direct red 28 azo dye by ozonation. Desalin. Water Treat 57:4135–4145
12. Guo J, Zhang Q, Cai Z, Zhao K (2016) Preparation and dye filtration property of electrospun polyhydroxybutyrate-calcium alginate/carbon nanotubes composite nanofibrous filtration membrane. Sep Purif Technol 161:69–79
13. Zou HM, Ma WZ, Wang Y (2015) A novel process of dye wastewater treatment by linking advanced chemical oxidation with biological oxidation. Arch Environ Prot 41:33–39
14. Makarchuk OV, Dontsova TA, Astrelin IM (2016) Magnetic nanocomposites as efficient sorption materials for removing dyes from aqueous solutions. Nanoscale Res Lett 11:161–161
15. Yao T, Guo S, Zeng C, Wang C, Zhang L (2015) Investigation on efficient adsorption of cationic dyes on porous magnetic polyacrylamide microspheres. J Hazard Mater 292:90–97
16. Chen Q, Wu Q (2015) Preparation of carbon microspheres decorated with silver nanoparticles and their ability to remove dyes from aqueous solution. J Hazard Mater 283:193–201
17. Walker GM, Weatherley LR (1997) Adsorption of acid dyes on to granular activated carbon in fixed beds. Water Res 31:2093–2101
18. Namasivayam C, Yamuna RT, Arasi D (2002) Removal of procion orange from wastewater by adsorption on waste red mud. Separ Sci Technol 37:2421–2431
19. Ranjithkumar V, Sangeetha S, Vairam S (2014) Synthesis of magnetic activated carbon/alpha-Fe_2O_3 nanocomposite and its application in the removal of acid yellow 17 dye from water. J Hazard Mater 273:127–135
20. Zubir NA, Yacou C, Motuzas J, Zhang X, JCD C (2014) Structural and functional investigation of graphene oxide-Fe_3O_4 nanocomposites for the heterogeneous Fenton-like reaction. Sci Rep 4:4594
21. Woo K, Hong J, Choi S, Lee HW, Ahn JP, Kim CS, Lee SW (2004) Easy synthesis and magnetic properties of iron oxide nanoparticles. Chem Mater 16:2814–2818
22. Wang N, Zhu L, Wang D, Wang M, Lin Z, Tang H (2010) Sono-assisted preparation of highly-efficient peroxidase-like Fe_3O_4 magnetic nanoparticles for catalytic removal of organic pollutants with H_2O_2. Ultrason Sonochem 17:526–533
23. Wang W, Liu Y, Li T, Zhou M (2014) Heterogeneous Fenton catalytic degradation of phenol based on controlled release of magnetic nanoparticles. Chem Eng J 242:1–9
24. Zhang Z, Kong J (2011) Novel magnetic Fe_3O_4@C nanoparticles as adsorbents for removal of organic dyes from aqueous solution. J Hazard Mater 193:325–329
25. Wang Y, Cheng R, Wen Z, Zhao L (2012) Facile preparation of Fe_3O_4 nanoparticles with cetyltrimethylammonium bromide (CTAB) assistant and a study of its adsorption capacity. Chem Eng J 181-182:823–827
26. Zhang YR, Wang SQ, Shen SL, Zhao BX (2013) A novel water treatment magnetic nanomaterial for removal of anionic and cationic dyes under severe condition. Chem Eng J 233:258–264
27. Pourjavadi A, Moghanaki AA, Nasseri SA (2016) A new functionalized magnetic nanocomposite of poly(methylacrylate) for the efficient removal of anionic dyes from aqueous media. RSC Adv 6:7982–7989

28. Elhabiri M, Carrer C, Marmolle F, Traboulsi H (2007) Complexation of iron(III) by catecholate-type polyphenols. Inorg Chim Acta 360:353–359
29. Stahl HG, Patrick A, Hogan II, Schmidt WL, Wall SJ, Buhrlage A, Bullen HA (2010) Surface complexation of catechol to metal oxides: an ATR-FTIR, adsorption, and dissolution study. Environ Sci Technol 44:4116–4121
30. Slikboer S, Grandy L, Blair SL, Nizkorodov SA, Smith RW, Abadleh HAA (2015) Formation of light absorbing soluble secondary organics and insoluble polymeric particles from the dark reaction of catechol and guaiacol with Fe(III). Environ Sci Technol 49:7793–7801
31. Faure E, Daudre CF, Jerome C, Lyskawa J, Fournier D, Woisel P, Detrembleur C (2013) Catechols as versatile platforms in polymer chemistry. Prog Polym Sci 38:236–270
32. Ye Q, Zhou F, Liu W (2011) Bioinspired catecholic chemistry for surface modification. Chem Soc Rev 40:4244–4258
33. Zhou LC, Shao YM, Liu JR, Ye ZF, Zhang H, Ma JJ, Jia Y, Gao WJ, Li YF (2014) Preparation and characterization of magnetic porous carbon microspheres for removal of methylene blue by a heterogeneous Fenton reaction, Acs Appl. Mater Inter 6:7275–7285
34. Avazpour L, Zandi khajeh MA, Toroghinejad MR, Shokrollahi H (2015) Synthesis of single-phase cobalt ferrite nanoparticles via a novel EDTA/EG precursor-based route and their magnetic properties. J Alloy Compd 637:497–503
35. Yadav RS, Havlica J, KuÅitka I, Kozakova Z, Palou M, Bartonkov E, Boh M, Frajkorov F, Masilko J, Kalina L (2015) Magnetic properties of dysprosium-doped cobalt ferrite nanoparticles synthesized by starch-assisted sol–gel autocombustion method. J Supercond Nov Magn 28:2097–2107
36. Zhang JW, Azam MS, Shi C, Huang J, Bin B, Liu QX, Zeng HB (2015) Poly(acrylic acid) functionalized magnetic graphene oxide nanocomposite for removal of methylene blue. RSC Adv 5:32272–32282
37. Li GY, Huang KL, Jiang YR, Ding P, Yang DL (2008) Preparation and characterization of carboxyl functionalization of chitosan derivative magnetic nanoparticles. Biochem Eng J 40:408–414
38. Luo S, Xu X, Zhou G, Liu C, Tang Y, Liu Y (2014) Amino siloxane oligomer-linked graphene oxide as an efficient adsorbent for removal of Pb(II) from wastewater. J Hazard Mater 274:145–155
39. Liu Y, Zeng G, Tang L, Cai Y, Pang Y, Zhang Y, Yang G, Zhou Y, He X, He Y (2015) Highly effective adsorption of cationic and anionic dyes on magnetic Fe/Ni nanoparticles doped bimodal mesoporous carbon. J colloid interf sci 448:451–459
40. Liu F, Jin Y, Liao H, Cai L, Tong M, Hou Y (2013) Facile self-assembly synthesis of titanate/Fe_3O_4 nanocomposites for the efficient removal of Pb^{2+} from aqueous systems. J Mater Chem A 1:805–813
41. Zhang YR, Su P, Huang J, Wang QR, Zhao BX (2015) A magnetic nanomaterial modified with poly-lysine for efficient removal of anionic dyes from water. Chem Eng J 262:313–318
42. Hu XB, Liu BZ, Deng YH, Chen HZ, Luo S, Sun C, Yang P, Yang SG (2011) Adsorption and heterogeneous Fenton degradation of 17 alpha-methyltestosterone on nano Fe_3O_4/MWCNTs in aqueous solution. Appl Catal B-Environ 107:274–283
43. Zhao L, Yu B, Xue F, Xie J, Zhang X, Wu R, Wang R, Hu Z, Yang ST, Luo J (2015) Facile hydrothermal preparation of recyclable S-doped graphene sponge for Cu^{2+} adsorption. J Hazard Mater 286:449–456
44. Xu J, Lv H, Yang ST, Luo J (2013) Preparation of graphene adsorbents and their applications in water purification. Rev Inorg Chem 33:139–160